THE JOURNAL OF PHYSICAL CHEMISTRY B

Article

pubs.acs.org/JPCB

Crowding-Induced Phase Separation of Lennard-Jones Particles: Implications to Nuclear Structures in a Biological Cell

Eun Jin Cho[†] and Jun Soo Kim[‡,*]

[†]Department of Chemistry and Applied Chemistry, Hanyang University, Ansan, Kyeonggi-do 426-791, Republic of Korea, and
[‡]Department of Chemistry and Nano Science, Ewha Womans University, Seoul 120-750, Republic of Korea

ABSTRACT: We investigate the phase separation of Lennard-Jones (LJ) particles in the presence of cosolute crowders using molecular dynamics simulations. In the absence of crowders, LJ particles phase-separate and form liquid and vapor phases only when the attraction between LJ particles is strong enough such that k_BT/ε is less than 1.085, where ε is the attraction strength of the LJ potential, k_B is the Boltzmann constant, and T is the temperature. On the other hand, the phase separation of LJ particles is observed even for larger k_BT/ε and thus for weaker attractions when volume exclusive, repulsive crowders are present. Although the impact of crowding becomes less significant as the attraction between crowders and LJ particles is increased, the phase separation observed from simulations containing both nonattractive and attractive crowders shows that the crowding-induced phase separation by nonattractive crowders is still very significant even *in the presence of other attractive crowders*. This occurs because not only LJ particles but also attractive crowders are subject to the excluded volume effect of nonattractive crowders and found together in the condensed phase. This study suggests that the excluded volume effect in the crowded nuclear environment may play a crucial role in the formation and maintenance of biological structures in a cell, such as nuclear bodies including nucleoli and cajal bodies.

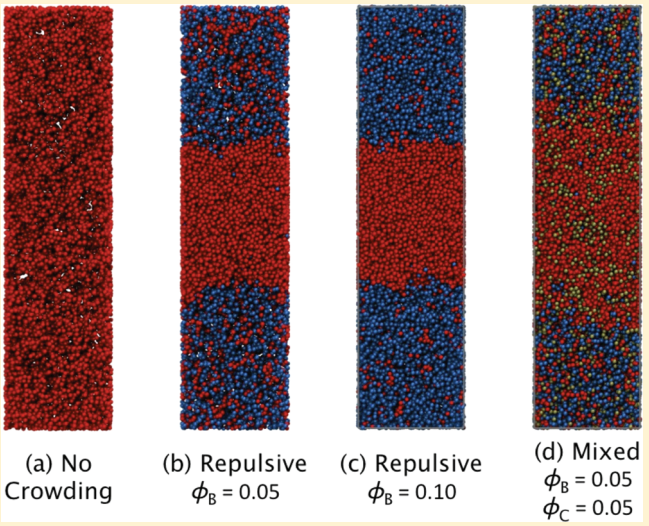

INTRODUCTION

A cell nucleus is crowded with a high content of macromolecules, and it was shown that this crowding plays an important role in compaction of chromatin fibers and formation of other nuclear structures such as nucleoli and cajal bodies.[1−7] The entropically driven depletion attraction induced between a pair of macromolecules due to crowding has been recognized as an important driving force for such structural alterations[1−3,6−10] and calculated for simple model systems.[7,8] However, it has not been directly examined how the depletion attractions can change the demixing behavior of structure-forming macromolecules and thus the structure formation in the crowded environment.

Nuclear bodies such as nucleoli, cajal bodies, and speckles are morphologically distinct structures observed in cell nuclei. Even though their functional roles in transcription, replication, and repair have been suggested,[11−13] the physics of structure formation and maintenance remains largely unknown. Recent studies have shown that nuclear bodies are formed by a random assembly of constituting proteins.[14,15] Since these proteins are known to self-interact to form the nuclear bodies[12,13] and they exist in crowded nuclear environments, it seems obvious that the macromolecular crowding should play an important role in the formation and maintenance of such nuclear bodies. In fact, a recent experimental study has shown that nucleoli and cajal bodies are dissembled under less crowded conditions and reassemble when the crowders are added.[2]

In this work, we investigate the phase separation of particles interacting through the Lennard-Jones (LJ) potential in the presence of crowders, with the goal of better understanding the role of crowding in the formation and maintenance of nuclear structures. The phase behavior of LJ particles has been studied extensively by theoretical and computational methods.[16−19] Since its phase behavior is well understood, LJ particles can serve as a prototypical model of a self-associating fluid, such as nuclear body proteins. The formation of nuclear bodies has some similarities with vapor−liquid phase separation of LJ particles. Nuclear body proteins can phase-separate into condensed and dilute phases and these phases are not separated by any physical boundary such as membranes. Thus, these macromolecules can be dynamically exchanged between

Received: January 19, 2012
Revised: February 29, 2012
Published: February 29, 2012

condensed and dilute phases, which are the common features seen in the vapor−liquid phase separation of LJ particles.

First, we address the question of how the phase separation of LJ particles will be affected due to the presence of purely repulsive, volume-exclusive crowders, since many experimental studies on crowding effects have been conducted using inert crowders such as dextran and poly(ethylene glycol).[2,5] Second, we investigate the effect of attractive crowders. In particular, we study a crowded system containing both purely repulsive crowders and attractive crowders. Many previous studies focused on the excluded volume effect of inert, nonattractive crowders as mentioned above, and therefore there have been concerns about neglecting the effect of attractive crowders.[10] Thus, the mixed crowding system (containing both repulsive crowders and attractive crowders) studied in this work can provide a useful information about the effect of crowding when attractive crowders also exist at a significant concentration.

For such purposes, we perform molecular dynamics (MD) simulations of systems containing a single component (only LJ particles without crowders), two components (either repulsive or attractive crowders with LJ particles), and three components (both repulsive crowders and attractive crowders together with LJ particles). For a given attraction strength of LJ particles or equivalently for a given temperature, we compare the demixing behavior of a single component system with those of multicomponent systems so that the effect of crowding on the phase separation of LJ particles is understood at the given condition. By varying the attraction strength of LJ particles (or the temperature), we determine its range for which the phase separation occurs, and the range for phase separation is compared between results of the single component system and those of the multicomponent systems. We believe such comparisons can help us figure out how important the macromolecular crowding is in the phase separation of biological structures and what consequences may result from the change in crowding conditions.

It needs to be mentioned that MD simulations in this work are performed at constant number of each component (N), volume (V), and temperature (T). The phase equilibria of binary LJ mixtures have been studied extensively by computer simulation methods such as Gibbs ensemble method and semigrand canonical ensemble method.[20−23] In those studies, the phase diagram is determined at constant pressure rather than at constant volume and presents the coexistence curve in terms of temperature and a mole fraction of one component in the liquid (or vapor) phase. However, in this work we run MD simulations at constant volume since the study of crowding effect usually focus on the structural and dynamical changes observed when the concentration (or the volume fraction) of crowders changes from one *fixed* value to the other value. In constant pressure simulations the system volume needs to be changed while keeping the pressure constant, and thus it changes the volume fraction of crowders in the system. This makes difficult the control of the crowder volume fraction at a fixed value and hinders the systematic investigation of the crowding-induced changes as a function of the crowder volume fraction. While *NVT*-simulation results in this work do not represent the phase diagram in a thermodynamic sense for multicomponent systems, it allows the systematic study of crowding effect at fixed volume fractions of different types of crowders.

The rest of this article is organized as follows: The models and simulation details are described in the next section. Simulation results are then discussed, and summary and conclusions are presented at the end.

METHODS AND MODELS

In this work the phase separation of LJ particles has been investigated by direct molecular dynamics (MD) simulations. We first perform simulations of a single component system containing identical LJ particles (called **A** particles hereafter). **A** particles interact with each other via the LJ potential $U_{AA}(r) = 4\varepsilon_{AA}[(\sigma/r)^{12} - (\sigma/r)^{6}]$, where ε_{AA} is the attraction strength between **A** particles and σ is the unit length. The potential is truncated and shifted at the cutoff radius of 2.5σ.

In the second set of simulations, we examine systems containing not only **A** particles but also cosolute crowding particles. Two types of crowders are studied in this work: crowders interacting via *purely repulsive* potentials with **A** particles as well as with other crowders (called **B** particles) and crowders interacting via *attractive* LJ potentials with both **A** particles and themselves (called **C** particles). Interaction potentials for crowders **B** and **C** are the same as that of **A** particles but with different attraction and cutoff parameters. The potentials are truncated and shifted at the cutoff radius of $2^{1/6}\sigma$ and 2.5σ for **B** and **C** crowders, respectively, so that the potentials of **B** crowders contain only the purely repulsive part of the LJ potential whereas those of **C** crowders also contain the attractive part of the LJ potential. For convenience, the attraction strength between **C** crowders and **A** particles is set the same as that between crowders themselves, that is, $\varepsilon_{AC} = \varepsilon_{CC}$.

All simulations are performed at constant N, V, and T, with GROMACS version 4.5.4.[24] The simulation system has an elongated cuboid-shaped dimension of $25\sigma \times 25\sigma \times 100\sigma$, containing 15 000 **A** particles and 5968 and 11937 crowders (either **B**, **C**, or a combination of both) for crowder volume fractions of 0.05 and 0.10, respectively. The number of **A** particles (corresponding to the reduced density of $\rho_A\sigma^3 = 0.24$) is chosen such that the thickness of the planar liquid phase (when the phase separation occurs) is about one-third of the simulation system along the z direction. The crowder volume fractions of 0.05 and 0.10 are chosen, since the protein density in the nucleoplasm of a specific cell of *Xenopus* oocyte is 0.106 g/cm^3 (the volume fraction is calculated as 0.077 using specific volume of 0.73 cm^3/g).[25] While higher volume fractions of crowders can be more relevant for other types of cells, the qualitative understanding will not change significantly but with more enhanced crowding effect. The crowder volume fractions are written, hereafter, as ϕ_B and ϕ_C for **B** and **C** crowders, respectively.

MD simulations are performed at a reduced temperature ($T^* = k_BT/\varepsilon_{AA}$) ranging between 0.65 and 1.60, where k_B is the Boltzmann constant and T is the temperature. Initial configurations for all sets of simulations are prepared by locating a thick layer of **A** particles in the middle of simulation system along the z direction. When crowders are present, **B** or **C** particles are distributed in the rest of the simulation volume. These configurations are used for simulations at the lowest temperature of 0.65 and the resulting configurations are used for the subsequent simulations at higher temperatures. Equations of motion are integrated using the leapfrog algorithm with a time step (δt) of $0.01\tau_{MD}$, where $\tau_{MD} = \sigma(m/\varepsilon_{AA})^{1/2}$. A total of 1.1×10^7 time steps ($1.1 \times 10^5\tau_{MD}$) is run for each simulation and the trajectories are stored every 10^3 time steps. The trajectories of 1×10^7 time steps after the equilibration in

dx.doi.org/10.1021/jp3006525 | J. Phys. Chem. B 2012, 116, 3874−3879

the first 1×10^6 time steps are used for calculation of equilibrium densities of dense and dilute phases.

For all sets of simulations, average density profiles of **A** particles at each k_BT/ε_{AA} are calculated along the elongated z direction, from which densities of dense and dilute phases are determined. When two phases coexist, the dense phase moves up and down along the z direction during simulation durations, and thus average density profiles are obtained by translating instantaneous density profiles such that the center of the dense phase is located at the center of simulation system ($z = 50\sigma$). The average density profiles calculated in such a way are symmetric around $z = 50\sigma$ and thus further averaged by superimposing the left and right halves of the density profiles. Then, densities of dense and dilute phases are obtained by fitting average density profiles to the equation

$$\rho(z) = \frac{1}{2}(\rho_l + \rho_v) - \frac{1}{2}(\rho_l - \rho_v)\tanh\frac{2(z-w)}{d} \quad (1)$$

where z is the coordinate along which the density profile is calculated, w is half the width of the dense phase, d is the interfacial thickness, and ρ_l and ρ_v are densities of dense and dilute phases, respectively.[19]

RESULTS AND DISCUSSION

Figure 1 shows snapshots of four simulated systems at $k_BT/\varepsilon_{AA} = 1.10$, in the absence of crowders (Figure 1a), in the presence of **B** crowders with volume fractions of 0.05 and 0.10 (Figure 1, parts b and c), and in the presence of mixed crowders of **B** and **C** particles with volume fractions of 0.05, respectively (Figure 1d). The snapshots are created using VMD.[26] At $k_BT/\varepsilon_{AA} = 1.10$, **A** particles in the absence of crowders form only a one phase fluid without phase separation. When **B** crowders (only with purely repulsive interactions) are added to the system, **A** particles phase-separate. As ϕ_B increases the phase separation becomes even clearer. In the case of mixed crowders, the phase separation is also observed although the condensation of **A** particles is not as sharp as in the presence of only **B** crowders. Figure 1 summarizes main results in this work and more details on each case are discussed below.

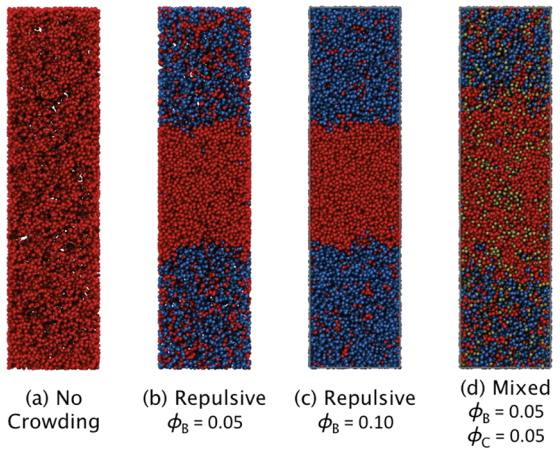

Figure 1. Representative snapshots of simulation systems at $k_BT/\varepsilon_{AA} = 1.10$. While the LJ particles (**A** particles, red) form a one phase fluid in the absence of crowders, the phase separation of **A** particles into high and low density phases are observed in the presence of crowders (**B** particles in blue and **C** particles in green). Figures are created by VMD.[26].

Phase Separation of A Particles in the Absence of Crowders. Average density profiles and the phase diagram are presented in Figure 2, parts a and b. Average density profiles at $k_BT/\varepsilon_{AA} < 1.10$ shows clear distinction between liquid and vapor phases. The interface is very narrow with a sharp transition between the two phases and the width of the liquid phase does not change significantly with varying k_BT/ε_{AA}. Densities of the liquid and vapor phases are calculated using eq 1. As k_BT/ε_{AA} increases, densities of the liquid phase decreases while that of the vapor phase increases until LJ particles form only a one fluid phase without phase separation, which corresponds to $k_BT/\varepsilon_{AA} \geq 1.10$.

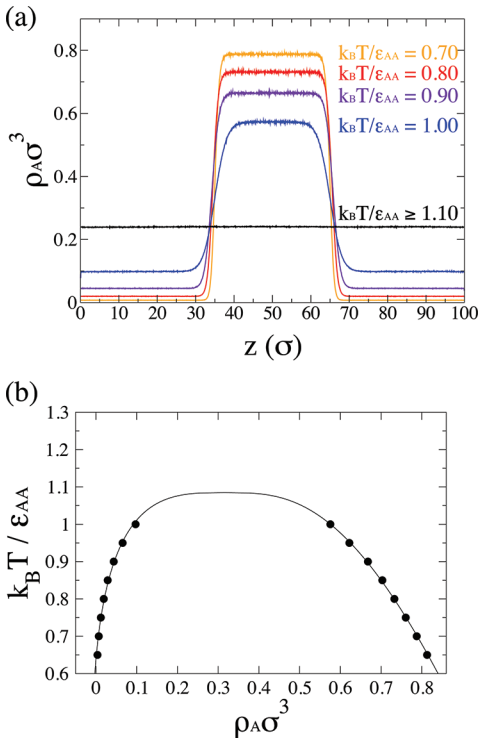

Figure 2. Phase separation of LJ particles (**A** particles) in the absence of cosolute crowders. (a) Density profiles of LJ particles along z direction for different k_BT/ε_{AA}. (b) The phase diagram of LJ particles depicting a range of the reduced temperature k_BT/ε_{AA} and the density $\rho_A\sigma^3$, in which the phase separation into high and low density phases occurs. The solid line in (b) is a fitting curve described in eqs 2 and 3.

Measured densities $\rho_A\sigma^3$ for liquid and vapor phases at each k_BT/ε_{AA} are depicted in the phase diagram shown in Figure 2b. The liquid/vapor critical temperature T_c can also be determined by fitting the measured densities to

$$\rho_l + \rho_v = a - bT \quad (2)$$

$$\rho_l - \rho_v = A(1 - T/T_c)^{0.318} \quad (3)$$

where a, b, and A are fitting parameters.[18] The critical temperature and the corresponding critical density are determined as 1.085 and 0.316, agreeing well with early MD simulation data.[18,19] Since the density of **A** particles is set at 0.24 ($\rho_A\sigma^3 = 0.24$), it can be predicted from the phase diagram that there occurs the phase separation as long as k_BT/ε_{AA} is less than ~1.085.

Phase Separation of A Particles in the Presence of Volume Exclusive, Purely Repulsive B Crowders. Figure 1

dx.doi.org/10.1021/jp3006525 | J. Phys. Chem. B 2012, 116, 3874–3879

shows that the phase separation of **A** particles is facilitated by the presence of **B** crowders: **A** particles do not phase-separate in the absence of **B** crowders, whereas the phase separation occurs in their presence. The facilitated phase separation by **B** crowders is depicted more clearly in Figure 3a where densities

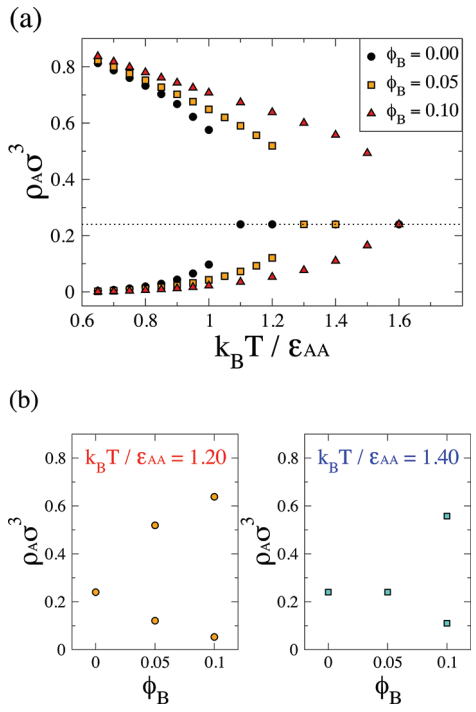

Figure 3. (a) Density of **A** particles as a function of k_BT/ε_{AA} in the absence and the presence of repulsive **B** crowders. Each symbol represents data for crowding volume fractions, ϕ_B = 0.00 (circles), 0.05 (squares), and 0.10 (triangles). Note that the two same symbols are presented for a single value of k_BT/ε_{AA} when there occurs the phase separation. A dotted line shows the total density of **A** particles ($\rho_A\sigma^3$ = 0.24). (b) Density of **A** particles as a function of the crowder volume fraction ϕ_B for k_BT/ε_{AA} = 1.20 and 1.40.

of **A** particles are presented as a function of k_BT/ε_{AA}. Each symbol in Figure 3 represents data for crowding volume fractions, ϕ_B = 0.00 (circles), 0.05 (squares), and 0.10 (triangles). The two identical symbols are presented for a single value of k_BT/ε_{AA} for a certain range of k_BT/ε_{AA}, which indicates the phase separation at those k_BT/ε_{AA}. In the absence of crowders (circles in Figure 3 (a)), the phase separation of **A** particles is observed when $k_BT/\varepsilon_{AA} < 1.10$, whereas a one phase fluid is observed at larger k_BT/ε_{AA}. However, in the presence of **B** crowders (rectangles and triangles in Figure 3a), the phase separation of **A** particles is observed even at k_BT/ε_{AA} larger than 1.10. The crowding-dependent phase separations at k_BT/ε_{AA} = 1.20 and 1.40 are presented in Figure 3b. At k_BT/ε_{AA} = 1.20, there exists a one phase fluid in the absence of crowders (ϕ_B = 0.00). However, for nonzero ϕ_B there occurs the phase separation with densities of dense and dilute phases whose difference becomes larger with increasing volume fraction. At k_BT/ε_{AA} = 1.40, the phase separation occurs only for ϕ_B = 0.10. This implies that the crowders can promote the phase separation of **A** particles even under the condition where it never occurs in the absence of crowders, that is, the phase separation occurs for weaker attractions between **A** particles. And the crowding-facilitated phase separation becomes more significant as ϕ_B increases.

Experimental data on the role of crowding in the maintenance of nuclear bodies can be interpreted based on data in Figure 3.[2] When cells were incubated in the media with low salt concentration, they became swollen and the nucleus became less crowded. In such cases, the nuclear bodies disappeared. However, nuclear bodies formed again when inert crowders such as dextran and poly(ethylene glycol) were added and the nuclear environment again became crowded. The attraction strength of nuclear body proteins ε_{AA} may not be large enough to form nuclear bodies in the absence of crowders, that is, k_BT/ε_{AA} may be greater than 1.10 so that the phase separation does not occur without crowders. When crowders are added and the nucleus becomes crowded, the phase separation occurs for larger values of k_BT/ε_{AA} or weaker attractions (rectangles and triangles in Figure 3). Therefore, the same attraction strength ε_{AA} is now large enough to form dense nuclear bodies due to crowding.

Phase separation of A particles in the presence of attractive C crowders. Nuclear proteins that behave as crowders may also have attractive interactions with nuclear body proteins. Therefore, we use crowders (**C** particles) that have attractive interactions with **A** particles as well as with themselves. Instead of considering multicomponent crowders with varying degrees of attractions, we first consider a single type of crowders with a mean attraction strength of ε_{XC}, where **X** can be either **A** or **C**. As shown in Figure 4a, the range of k_BT/ε_{AA} for phase separation also increases slightly when ε_{XC} is

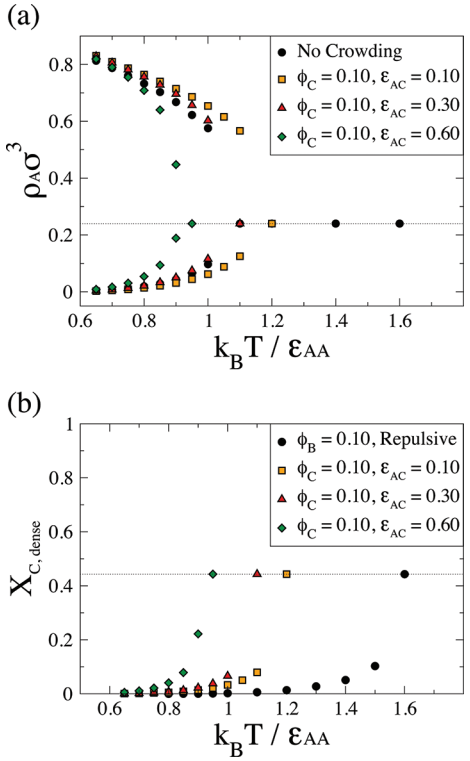

Figure 4. (a) Density of **A** particles as a function of k_BT/ε_{AA} in the absence and the presence of attractive **C** crowders. Each symbol represents data for $\varepsilon_{AC} = 0.10k_BT$ (squares), $0.30k_BT$ (triangles), and $0.60k_BT$ (diamonds). The attraction strength between **A** and **C** and that between **C** particles are set the same, that is, $\varepsilon_{AC} = \varepsilon_{CC}$. (b) Mole fraction of crowders in the dense phase as a function of k_BT/ε_{AA}. The dotted line is the total mole fraction of crowders 0.443 at the volume fraction of 0.10.

dx.doi.org/10.1021/jp3006525 | J. Phys. Chem. B 2012, 116, 3874−3879

$0.10k_BT$. However, as the attraction strength of the **C** crowders (ε_{XC}) is increased, the crowding effect on the formation of a dense phase of **A** particles is diminished, and when the attraction strength exceeds $0.30k_BT$, the range of k_BT/ε_{AA} for phase separation becomes even smaller. This result is predictable since as the attraction between **A** and **C** particles increases, **A** particles become more soluble in a solution of **C** crowders and vice versa. This interpretation is reflected in the change of the mole fraction of crowders with k_BT/ε_{AA} in Figure 4b. The mole fraction of **C** crowders (with $\varepsilon_{XC} = 0.60k_BT$) increases quickly after $k_BT/\varepsilon_{AA} = 0.85$ while that of **B** crowders is negligible until it reaches $k_BT/\varepsilon_{AA} = 1.50$.

This behavior with strong attractors is relevant to a recent experiment where the phase separation of monoclonal antibodies is shown to be suppressed in the presence of human serum albumin.[27] However, the results obtained when the mean attraction strength greater than $0.30k_BT$ is not in agreement with the crowding experimental results,[2] where the formation of nuclear bodies is stabilized by crowding, and therefore simulations containing only **C** crowders with a strong mean attraction do not seem to represent the crowding behavior occurring in the nuclear environment. In the following study, therefore, we use two crowders together in the simulation system, one with strong attraction of $\varepsilon_{XC} = 0.60k_BT$ and the other with no attraction.

Phase Separation of A Particles in the Case of Mixed Crowding with both Nonattractive B Crowders and Attractive C Crowders. Many nuclear proteins and their relative locations have been identified.[28] There are proteins categorized as diffuse proteins which are likely to be found in the nucleoplasm rather than associated with chromosomes or other nuclear bodies. Therefore, these proteins should be less attractive to nuclear bodies. Thus, while some nuclear proteins may have significant attractions with nuclear bodies, others may be weakly attractive or nonattractive to nuclear bodies. On the basis of this, we examine the effect of a collection of purely repulsive and attractive crowders on phase behavior. Here both crowders of **B** and **C** particles are included in the simulation system. The total volume fraction of both crowders is maintained at 0.10. Half of the crowders interact via the LJ potential with ε_{AC} and ε_{CC} of $0.60k_BT$ (**C** crowders) and the other half interact purely repulsively with **A** particles (**B** crowders). Naively, we expected that the phase diagram might be close to that in the presence of only **C** crowders with $\varepsilon_{XC} = 0.30k_BT$ which might be considered as the mean value of attraction strengths of nonattractive crowders and attractive crowders with $\varepsilon_{XC} = 0.60k_BT$. Interestingly, the effects of mixed crowders are very distinct from that of only **C** crowders.

In Figure 5a, densities of **A** particles as a function of k_BT/ε_{AA} in the presence of mixed crowders are compared with those of **A** particles in the absence of any crowders. The range of k_BT/ε_{AA} for phase separation is clearly extended to higher values, implying that the mixed crowders also promote the phase separation of **A** particles. Comparison of the **A** particle densities in the case of mixed crowding (rectangles) with those of only **C** crowders with $\varepsilon_{XC} = 0.30k_BT$ (Figure 4) shows that the effect of mixed crowders is different from that of **C** crowders interacting with a mean attraction strength. It seems that to model various crowders with a single type of interacting particles with mean attraction strength is not a good approach to study the crowding effect in polydisperse biological environments.

Although densities of two phases are clearly different from each other up to $k_BT/\varepsilon_{AA} = 1.20$ in Figure 5a, the difference

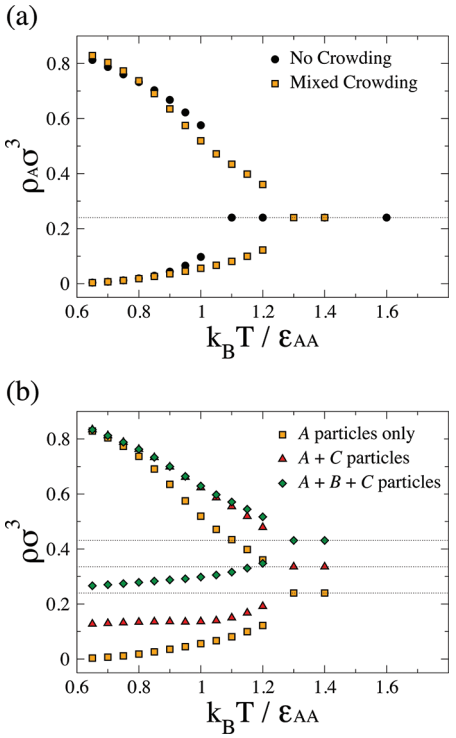

Figure 5. (a) Comparison of **A** particle densities as a function of k_BT/ε_{AA} in the absence and presence of mixed crowders (**B** + **C** particles). (b) Densities of **A** particles only, **A** + **C** particles, and **A** + **B** + **C** particles as a function of k_BT/ε_{AA}. Here, $\varphi_B = \varphi_C = 0.05$, so that the total volume fraction is equal to 0.10. Dotted lines at $\rho\sigma^3 = 0.24$, 0.34, and 0.43 are the total densities of **A**, **A** + **C**, and **A** + **B** + **C** particles, respectively.

between the densities of dense and dilute phases is rather small with increasing k_BT/ε_{AA} in the case of mixed crowding. This is because not only **A** particles but also a significant number of **C** particles are also present in the dense phase as shown in Figure 1d. Densities of two phases including crowders are depicted again for the mixed crowding in Figure 5b. At small k_BT/ε_{AA}, the **B** and **C** crowder densities are negligible in the dense phase and high in the low density phase. This occurs because the attraction between **A** particles is so strong that crowders are mostly excluded from the dense phase. However, when k_BT/ε_{AA} is increased to more than 0.85, the attractive **C** particles are also found frequently in the dense phase such that its density becomes slightly greater in the dense phase than that in the low density phase. This can be interpreted as the crowding effect of nonattractive **B** crowders. We also perform additional simulations of the system containing only **C** crowders (with $\varepsilon_{XC} = 0.60k_BT$) at $\phi_C = 0.05$ and it is found that the phase separation occurs only up to $k_BT/\varepsilon_{AA} = 0.95k_BT$ (data not shown). The phase separation observed between $k_BT/\varepsilon_{AA} = 1.00k_BT$ and $1.20k_BT$ for the mixed crowding is clearly the consequence of the presence of the nonattractive **B** crowders. Here, not only **A** particles but also **C** particles are subject to the excluded volume effect of nonattractive **B** crowders, and therefore more **C** particles are found in **A**-rich dense phase.

The significant density of **C** crowders in the dense phase is interesting when interpreted for nuclear bodies. Although some essential proteins forming the nuclear bodies are known,[14] the compete list of proteins forming the nuclear bodies is not available at the moment. It can be inferred from the significant density of **C** crowders in the dense phase that there might be

dx.doi.org/10.1021/jp3006525 | J. Phys. Chem. B 2012, 116, 3874−3879

some nonessential and nonspecific proteins that are contained in the nuclear bodies by crowding effect.

CONCLUSIONS

In conclusion, the phase separation and thus self-association of LJ particles is significantly promoted in the crowded environment. The facilitated phase separation induced by the presence of volume exclusive, repulsive crowders is adopted to explain the experimental observation of crowding-controlled nuclear body formation. Such crowding-induced phase separation is diminished by the attraction between crowders and LJ particles. Interestingly, however, the phase separation is still promoted significantly in the case of mixed crowding where the concentration of attractive crowders is as large as that of nonattractive crowders. Therein, the excluded volume effect induced by nonattractive crowders is shown to alter the density of attractive crowders as well as that of LJ particles (**A** particles) in the two phases. In this case, attractive crowders are also contained in the **A**-rich dense phase. It might be inferred from the significant density of attractive crowders in the dense phase that there might be some nonspecific proteins that are contained in the nuclear bodies due to crowding.

In the nuclear environment, there are a variety of proteins that have varying degrees of interactions with nuclear bodies. It is reasonable to assume that some of those nuclear proteins have weak or no attraction with nuclear body proteins. These nonattractive proteins are expected to promote the self-association of nuclear body proteins and should play an important role in the formation and maintenance of nuclear bodies. In this study, simple LJ particles are employed to model the self-associating fluid. Identifying biologically relevant proteins and developing more realistic models will be pursued in future efforts. However, this simple model provides physical insights into the effect of crowding on the formation and maintenance of nuclear bodies in terms of the enlarged range of attraction strength that induces phase separation in the presence of cosolute crowders.

AUTHOR INFORMATION

Corresponding Author

*E-mail: jkim@ewha.ac.kr.

Notes

The authors declare no competing financial interest.

ACKNOWLEDGMENTS

This research was supported by the National Research Foundation of Korea (NRF) under Grant NRF-2011-0024621. This work was also supported by the National Research Foundation of Korea (NRF) under Grant NRF-2011-220-C00030, and by the Ewha Global Top 5 Grant 2011 of Ewha Womans University.

REFERENCES

(1) Zimmerman, S. B. *Biochim. Biophys. Acta* **1993**, *1216*, 175−185.
(2) Hancock, R. *J. Struct. Biol.* **2004**, *146*, 281.
(3) Finan, K.; Cook, P. R.; Marenduzzo, D. *Chromosome Res.* **2011**, *19*, 53−61.
(4) Albiez, H.; et al. *Chromosome Res.* **2006**, *14*, 707−733.
(5) Richter, K.; Nessling, M.; Lichter, P. *J. Cell Sci.* **2007**, *120*, 1673−1680.
(6) Kim, J. S.; Backman, V.; Szleifer, I. *Phys. Rev. Lett.* **2011**, *106*, 168102.
(7) Marrenduzzo, D.; Micheletti, C.; Cook, P. R. *Biophys. J.* **2006**, *90*, 3712−3721.
(8) Kim, J. S.; Szleifer, I. *J. Phys. Chem. C* **2010**, *114*, 20864−20869.
(9) Kim, J. S.; Yethiraj, A. *J. Phys. Chem. B* **2011**, *115*, 347−353.
(10) Zhou, H.-X.; Rivas, G.; Minton, A. P. *Annu. Rev. Biophys.* **2008**, *37*, 375−397.
(11) Misteli, T. *Cell* **2007**, *128*, 787−800.
(12) Matera, A. G.; Izaguire-Sierra, M.; Praveen, K.; Rajendra, T. K. *Dev. Cell* **2009**, *17*, 639−647.
(13) Brangwynne, C. P. *Soft Matter* **2011**, *7*, 3052−3059.
(14) Kaiser, T. E.; Intine, R. V.; Dundr, M. *Science* **2008**, *322*, 1713−1717.
(15) Misteli, T. *Nature* **2008**, *456*, 333−334.
(16) Panagiotopoulos, A. Z. *Mol. Phys.* **1987**, *61*, 813.
(17) Johnson, J. K.; Zollweg, J. A.; Gubbins, K. E. *Mol. Phys.* **1993**, *78*, 591−618.
(18) Sides, S. W.; Grest, G. S.; Lacasse, M. *Phys. Rev. E* **1999**, *60*, 6708−6713.
(19) Vrabec, J.; Kedia, G. K.; Fuchs, G.; Hasse, H. *Mol. Phys.* **2006**, *104*, 1509−1527.
(20) Georgoulaki, A. M.; Ntouros, I. V.; Tassios, D. P.; Panagiotopoulos, A. Z. *Fluid Phase Equilib.* **1994**, *100*, 153.
(21) Vlot, M. J.; van Miltenburg, J. C.; Oonk, H. A. J.; van der Eerden, J. P. *J. Chem. Phys.* **1997**, *107*, 10102−10111.
(22) Mecke, M.; Winkelmann, J.; Fischer, J. *J. Chem. Phys.* **1999**, *110*, 1188−1194.
(23) Lamm, M. H.; Hall, C. K. *Fluid Phase Equilib.* **2001**, *182*, 37−46.
(24) van der Spoel, D.; Lindahl, E.; Hess, B.; Groenhof, G.; Mark, A. E.; Berendsen, H. J. C. *J. Comput. Chem.* **2005**, *26*, 1701.
(25) Handwerger, K. E.; Cordero, J. A.; Gall, J. G. *Mol. Biol. Cell* **2005**, *16*, 202−211.
(26) Humphrey, W.; Dalke, A.; Schulten, K. *J. Mol. Graphics* **1996**, *14*, 33−38.
(27) Wang, Y.; Lomakin, A.; Latypov, R. F.; Benedek, G. B. *Proc. Natl. Acad. Sci. U.S.A.* **2011**, *108*, 16606−16611.
(28) Bickmore, W. A.; Sutherland, H. G. E. *EMBO J.* **2002**, *21*, 1248−1254.

NOTE ADDED AFTER ASAP PUBLICATION

This paper was published ASAP on March 12, 2012. The caption to Figure 2 was updated. The revised paper was reposted on March 19, 2012.